DOI:
10.1088/0957-4484/27/49/494004

Document Version
Peer reviewed version

Journal Name

ARTICLE

Light-activated control of protein channel assembly mediated by membrane mechanics

Received 00th January 20xx,
Accepted 00th January 20xx

DOI: 10.1039/x0xx00000x

www.rsc.org/

David M Miller[a,b], Heather E Findlay[c], Oscar Ces[d], Richard H Templer[d], and Paula J Booth[c]

Photochemical processes provide versatile triggers of chemical reactions. Here, we use a photoactivated lipid switch to modulate the folding and assembly of a protein channel within a model biological membrane. In contrast to the information rich field of water-soluble protein folding, there is only a limited understanding of the assembly of proteins that are integral to biological membranes. It is however possible to exploit the foreboding hydrophobic lipid environment and control membrane protein folding via lipid bilayer mechanics. Mechanical properties such as lipid chain lateral pressure influence the insertion and folding of proteins in membranes, with different stages of folding having contrasting sensitivities to the bilayer properties. Studies to date have relied on altering bilayer properties through lipid compositional changes made at equilibrium, and thus can only be made before or after folding. We show that light-activation of photoisomerisable di-(5-[[4-(4-butylphenyl)azo]phenoxy]pentyl)phosphate (4-Azo-5P) lipids influences the folding and assembly of the pentameric bacterial mechanosensitive channel MscL. The use of a photochemical reaction enables the bilayer properties to be altered during folding, which is unprecedented. This mechanical manipulation during folding, allows for optimisation of different stages of the component insertion, folding and assembly steps within the same lipid system. The photochemical approach offers the potential to control channel assembly when generating synthetic devices that exploit the mechanosensitive protein as a nanovalve.

Introduction

Protein folding is fundamental to protein function but the precise nature of this essential reaction, in which the linear amino sequence folds to the singular active three-dimensional structure, remains to be fully understood. The mechanisms of folding and assembly of oligomeric, integral membrane proteins are particularly obscure as attention has been focussed on water-soluble proteins. However, despite the innate difficulties in working with membrane proteins their lipid neighbours offer an advantage over an aqueous surrounding, with the chance to manipulate the solvent in a controlled manner to modulate membrane protein folding. Here, we exploit the mechanical properties of the lipid bilayer to trigger membrane assembly reactions using lipid photoisomerisation to modulate the physical attributes of the lipid membrane. This provides a generic triggering method, targeting the common bilayer that surrounds integral membrane proteins.

Biological lipids regulate many natural processes. The interaction of an integral membrane protein with lipids is complex and consists of direct interactions, as well as non-specific interactions arising from the physical and mechanical properties of the bilayer [1-7]. Many membrane proteins, including a number of transmembrane α helical channels, function as homo-oligomers. There is evidence to suggest some of these proteins may change oligomeric state as a result of movement through different membrane systems within the cell [8, 9]. The intricacy of cell membranes that contain many different lipids and proteins makes it challenging to elucidate the roles of non specific, collective membrane properties. Nonetheless, such properties can be readily exploited in synthetic systems, for which knowledge of lipid phase and mechanical properties enables protein reactions to be controlled and correlated with lipid parameters. Bilayer mechanics have been shown to influence the folding of membrane proteins [3, 4, 10-12]. In particular, the lateral pressure exerted on the protein by the lipids in the x-y plane of the bilayer has been linked directly to helix insertion, packing and protein stability. Lipid lateral pressure depends on depth in the monolayer; thus there are usually outward positive pressures in the lipid headgroup and chain regions that are offset by a sharp inward negative pressure at the interfacial

[a] The Walter and Eliza Hall Institute of Medical Research, Parkville, Victoria 3052, Australia.
[b] Department of Medical Biology, The University of Melbourne, 3052, Australia.
[c] Department of Chemistry, King's College London, 7 Trinity Street, London SE1 1DB, UK.
[d] Department of Chemistry and Institute of Chemical Biology, Imperial College London, Exhibition Road, London SW7 2AZ, UK.

region. Lipid chain pressure can be significant and increases with increasing unsaturation in the lipid chain. A high outward chain pressure in the centre of the bilayer increases the activation energy for transmembrane helix insertion, which results in a reduction in the amount of inserted, functional protein [13] [14]. Previous studies on lipid effects on folding have focussed on bacteriorhodopsin [15-17], *Escherichia coli* diacylglycerol kinase [18, 19], lactose permease [20, 21] and the potassium channel KcsA [22-24]. Here, we add the pentameric mechanosensitive channel, MscL to this currently rather limited list.

MscL is a membrane channel that functions as a valve in bacteria responding to changes in membrane tension and preventing lysis under osmotic shock. The response to membrane tension of MscL channel opening has been studied in synthetic lipid mixtures and a direct dependence was found for the free energy of the open state on lipid monolayer spontaneous curvature [25, 26]. The functional state of MscL is thought to be a homopentamer with each monomer having two transmembrane helices and a third cytoplasmic helix (Fig 1). There is evidence for multiple oligomeric states of the channel, ranging from tetramers to hexamers, partly depending on the C-terminal domain and solubilisation conditions *in vitro* [27, 28]. The published homologous *Mycobacterium tuberculosis* crystal structure of MscL is a pentamer [29]; a pentamer was observed by electron microscopy [30] and atomic force microscopy [31] and work involving tandem repeat constructs of MscL showed the functional oligomer to be the pentamer[32]. A structure of a C-terminal truncated form of *Staphylococcus aureus* MscL revealed a tetramer in a partially opened form [33]. This MscL was found to be pentameric *in vivo*, with the C-terminal domain playing a role in the oligomeric state when solubilised in detergent [28].

The work here demonstrates that not only does channel function respond to changes in bilayer mechanics, but channel assembly is also mechanosensitive. *In vivo* the *E. coli* MscL channel is thought to insert without the involvement of the translocon but possibly with the assistance of an another membrane protein, YidC. MscL can, however, insert spontaneously into bilayers without YidC *in vitro* [34, 35]. We have utilised this spontaneous insertion ability to develop a method to fold partly denatured MscL into a lipid bilayer and instigate the use of photoactive lipids to modulate channel assembly. Protein Tryptophan (Trp) fluorescence is used to follow refolding, together with inter-monomer fluorescence energy transfer (i.e. Förster resonance energy transfer, FRET) and fluorescence quenching to monitor monomer association. Photoisomerisation of 4-azo-5P lipids (see Fig S1) is used to initiate changes in bilayer properties. Complete isomerisation of these azo lipids is readily determined by changes in the absorbance spectrum of the azo lipids (see Fig S2). Previously, channel gating has been shown to be modulated by this photoisomerisation, with isomerisation from *trans* to *cis* azo lipids activating MscL[36]. The activation results from the changes induced in the membrane bilayer physico-chemical properties upon lipid isomerisation. The *trans* and *cis* forms of the lipids adopt different conformations in bilayers and converting between the two isomers alters bilayer properties. It has previously been shown that isomerisation from the *trans* to *cis* state of these azo lipids in phosphytidylcholine (PC) vesicles results in an increase in chain disorder for the *cis* state and a significant disturbance in chain packing that affects the ordering of the neighbouring PC lipids. There is no change in bilayer thickness, nor to vesicular shape when the azo lipid concentrations are <16mol%, whereas at concentrations >50mol% isomerisation to the *cis* state results in sheet structures [37, 38]. Such changes in chain disorder are consistent with an increase in chain lateral pressure when the *cis* state of the azo lipids is present. This state reverts to the more stable *trans* state over time at room temperature.

Here, we show control of channel assembly by altering the lipid bilayer physical properties, during the folding reaction, through azo lipid photoisomerisation. Channel gating of MscL has also been manipulated by attachment of a photochemical group to the protein, as well as the introduction of charged amino acids [39]. Taken together this provides a useful synthetic system, whereby a protein channel valve can be controlled directly or indirectly via the lipid bilayer, with both assembly and channel gating being modulated by a photochemical switch.

Results

Refolding MscL into detergent micelles and lipid vesicles

MscL was initially refolded into dodecylmaltoside (DDM‡) detergent micelles. MscL was purified in DDM and denatured in mixed DDM/SDS micelles, containing up to 8 mM SDS. The channel was subsequently re-assembled from this sodium dodecylsulfate (SDS)-denatured state (referred to as MscL-SDS). SDS dissociated the intact, DDM-solubilized MscL pentamer and induced partial unfolding. Far UV circular dichroism (CD) studies showed a reduction in α helical content from ~66 % in the pentamer to ~55 % in 0.87 mole fraction SDS (see Fig 2a-c), which is equivalent to approximately 16 residues per monomer losing helical structure (compared to a total of ~81 residues forming helices in each monomer in the closed structure; Fig 1 [29]). SDS-polyacrylamide gel electrophoresis (PAGE) and analytical ultracentrifugation (AUC) showed that the MscL pentamer was dissociated in SDS (see Fig S3 and Table S1; experimental conditions for measurements in this work are shown in table S2 for clarity and comparison).

The SDS-MscL state was refolded by dilution into DDM micelles, to a final SDS concentration of 3mM, just below the critical micelle concentration. Fig 2 b and c shows that the original secondary structure was fully recovered upon refolding into DDM, as determined from the characteristic α helical band at 222 nm.

FRET was used to follow pentamer dissociation and re-assembly (see Fig 2d). MscL monomers with a single Cys introduced at position 42 on the periplasmic loop localised between transmembrane helix 1 and 2 were labelled with either the

fluorophore Alexa-488 (donor) or Alexa-568 (acceptor) [40] (see Fig 1). No FRET was observed at high SDS (>8 mM), when SDS-PAGE and AUC showed that MscL was monomeric and thus dissociated. Thus, this loss of FRET is consistent with complete dissociation of the pentamer into isolated monomers. In contrast, FRET was observed after re-assembly, by dilution of SDS into DDM. Thus, the CD and FRET data for SDS-MscL refolded by dilution into DDM micelles indicate that there is complete recovery of helical structure and FRET. It also shows that the Alexa-labelled M42C mutant of MscL re-folds to the pentamer.

The SDS-MscL was also refolded, by dilution, into lipid vesicles consisting of 50 mol% L-α-1,2-dioleoyl-sn-glycero-3-phosphoglycerol (DOPG) and 50 mol% L-α-1,2-dioleoyl-sn-glycero-3-phosphocholine (DOPC). This lipid mixture was chosen since MscL activity is dependent upon lipid composition and this mixture gives optimal activity when compared to other DOPC/DOPG compositions. FRET was used to follow the refolding and assembly from SDS into PC/PG vesicles. The FRET spectrum of the folded and assembled MscL(M42C-Alexa) in PC/PG vesicles (Fig S4a) was determined by reconstitution of intact, purified MscL(M42C-Alexa) in DDM into the vesicles (ie the MscL was not denatured). Refolding of the SDS-induced monomeric MscL(M42C-Alexa) into PC/PG vesicles resulted in recovery of this original FRET spectrum. This suggests that refolding occurs to the pentameric starting complex. The FRET measurements in vesicles were made at equilibrium, of the final assembled state, after a sucrose flotation assay to separate the re-assembled MscL associated with the vesicles from any protein aggregates that influence the FRET spectra. The observed assembly of MscL in vesicles was concentration dependent, consistent with more efficient assembly of the pentameric state at higher concentrations of MscL. If the FRET spectrum in lipid vesicles is solely due a re-assembled pentamer, this would indicate that 72 ± 5 % of MscL assembled as a pentamer after refolding with an MscL mole fraction of 0.0016 (625 lipids per MscL monomer or 28 pentamers per lipid vesicle; see Fig S5a).

MscL function was monitored with a previously well-characterised assay [41, 42] in which chemical modification of a G22C MscL mutant with trimethylammonium ethyl methanethiosulfonate (MTSET) results in spontaneous channel opening. This assay has previously been shown to report high activity of MscL in PC/PG lipid mixtures, with the presence of PG increasing activity over purely zwitterionic vesicles [42]. In this activity assay, channel opening releases calcein dye from within the vesicles, which is measured as an increase in calcein fluorescence due to the reduction in calcein self-quenching within the vesicles[42, 43]. Importantly, this assay enables channel opening to be studied under the same conditions as used for the MscL folding experiments. Calcein dye release was monitored for MscL(G22C) refolded from SDS into PC/PG vesicles. Fig 3 shows that more calcein is released as the concentration of MscL(G22C) is increased, with ~21 % calcein released from lipid vesicles when ~72% of MscL re-assembles as pentamer (determined by FRET as described above). This degree of channel opening is in line with previous work on reconstituted active MscL giving approximately 25 % calcein release [42]. This is consistent with the majority of the MscL being re-assembled correctly into a functional state similar to that for purified, reconstituted channels and that the FRET is a reasonable measure of MscL re-assembly. The calcein assay showed, as expected, that more functional channels were observed when more MscL was folded into lipid vesicles (Fig S5b). Moreover, the observed activity directly correlated with the amount of functional channels observed by FRET (Fig S5c), again suggesting FRET is measuring functional MscL. Refolding in PC/PG vesicles as reported by FRET was similar for MscL (M42C-Alexa) and (M42C-Alexa G22C) mutants.

Refolding MscL into azolipid vesicles

SDS-denatured MscL was re-assembled by dilution into lipid vesicles containing azolipids; with the vesicles consisting of 40% DOPC, 50% DOPG and 10% azolipid (with a consistent 50% proportion of PG, unless otherwise stated). Two measures were used to follow the changes occurring upon refolding; Trp fluorescence quenching as well as FRET. MscL has no native Trp residues, so a non-native single Trp mutant, F93W, of MscL was used that has a Trp incorporated in the middle of transmembrane helix 2 (see Fig 1). F93W MscL exhibits channel activity similar to the native protein [41]. Changes in the fluorescence of this Trp upon refolding report upon the association of MscL with 4-Azo-5P containing lipid vesicles; the azo groups quench Trp fluorescence, as the absorption band of the azo group at 330-350 nm overlaps with the Trp emission band (see Fig 4).

MscL(F93W) was refolded from SDS into PC/PG vesicles containing either *cis* or *trans* azo lipids. The F93W fluorescence completely quenched upon folding SDS-MscL(F93W) into vesicles containing 2.5 % *trans* azo-lipids (and 47.5 % DOPC and 50 % DOPG; see Fig 4a). The *trans* state of the azo lipids is the lower energy state at room temperature and the *cis* lipids revert back to the *trans* state over time (slowly, >30 min). The magnitude of Trp fluorescence quenching in vesicles containing *cis* or *trans* lipids was also determined from kinetic data (reported in the following section), since steady-state spectra cannot be obtained for vesicles with *cis* lipids due to the partial re-isomerisation back to *trans* during the measurement. The time-resolved data circumvents this reversion to *trans* and showed that the F93W Trp fluorescence was completely quenched in both azo isomers. The quenching was determined to be complete; 103.8 ± 1.8 % and 106.6 ± 1.9 % for 50:50 PC/PG lipid vesicles containing 10 % *trans* and *cis* azo lipids, respectively. This is consistent with complete association or insertion of MscL with the 4-Azo-5P containing vesicles.

FRET was used to assess monomer association into an assembled oligomeric state, after refolding SDS-MscL(M42C-Alexa) into lipid vesicles containing 10 % 4-azo-5P in either *cis* or *trans* conformations. As previously, FRET spectra of the re-assembled state were recorded at equilibrium, after a sucrose

flotation assay to separate re-assembled MscL from protein aggregates. The *cis* azo isomer will partially revert to the more stable *trans* state during this sucrose flotation assay (but after refolding has occurred). Thus, although MscL was originally folded into vesicles containing either the *cis* or *trans* state, the final FRET measurement was recorded when the lipids had fully reverted back to *trans* to ensure consistency in measurements. The FRET spectra of re-assembled MscL in PC/PG/azo lipids were the same as that in PC/PG lipids (see Fig S4) consistent with functional pentameric MscL being recovered in vesicles with azolipids. A larger FRET signal was observed after folding SDS-MscL(M42CAlexa) into vesicles containing 10 % *trans*, as opposed to 10 % *cis*, 4-azo-5P, suggesting greater monomer, monomer association and pentamer formation with *trans* azolipids present during the refolding reaction (see Fig 5a).

Fig S4 shows control measurements that indicate the azo-lipid isomerization state does not influence the final conformation state of MscL, as reported by these FRET spectra. FRET was measured for MscL that has been reconstituted into lipid vesicles (ie already folded when transferred to the vesicle; there is no refolding). Fig S4 shows FRET spectra for DOPC/DOPG vesicles containing azo-lipid in 3 conditions: i) MscL reconstituted into vesicles containing *trans* lipids; ii) MscL reconstituted into *trans* lipids, which are then photoisomerised to *cis* and then back to *trans* for measurement and iii) MscL reconstituted into *cis*, which are photo-isomerised to *trans* for measurement. All spectra are the same, and are identical to the FRET spectrum for MscL reconstituted in DOPC/DOPG vesicles without any azo-lipid present. This indicates that there is no influence of switching the lipid isomerisation on the FRET spectra when MscL is always correctly assembled. Thus, the changes seen in the FRET (Fig. 5a) when MscL is folded into *trans* lipids as opposed to *cis* lipids are due to the azo-lipid isomerisation state affecting folding.

The activity of MscL in vesicles with azo lipid was verified after refolding into *cis* or *trans* 4-azo-5P containing lipid vesicles by calcein dye release. In this case, flotation assays were not used since aggregated protein does not affect the dye release. Hence, the determined activities are for MscL folded, and measured, in vesicles containing *cis* lipids, or MscL folded into and subsequently measured in *trans* lipids. The final resultant activity was similar, ~17-18%, for both *trans* and *cis* azolipids (Fig 5b). This is despite the apparent decrease in the amount of MscL that assembles in *cis* lipids as compared to *trans*, as shown by the FRET studies of the final end product after folding. An interpretation of this is that less functional MscL is recovered when folding is initiated into vesicles with *cis* azo lipids, but the recovered protein has increased activity in *cis* lipids resulting in equivalent dye release overall. This is consistent with more efficient assembly in *trans* compared to *cis*, but greater activity in *cis* compared to *trans*. This difference in activity between the different isomeric states is in agreement with previous work where MscL activity was found to be greater in the presence of the *cis* as opposed to *trans* azo lipid isomer [36].

Kinetics of MscL refolding into azo lipids

SDS-MscL was refolded into DOPC/DOPG lipid vesicles containing 10% azo lipid in the *cis* or *trans* conformation. The associated refolding kinetics were monitored upon stopped-flow mixing of SDS-MscL with vesicles, by time-resolving changes in: i) the fluorescence quenching of F93W (see Fig 1 and 4b), which reports primarily on association and insertion of MscL with vesicles (as the azo lipid quenches Trp fluorescence), as well as self-quenching of the F93W residues during monomer association; ii) azolipid quenching and self-quenching of rhodamine attached to M42C, which being in a loop region and in the aqueous phase reports mainly on monomer, monomer interactions of MscL and iii) FRET, which reports primarily on MscL monomer, monomer interactions and pentamer formation.

The Trp fluorescence decays of MscL F93W that were observed upon refolding, fit well to the sum of two or three first order exponential components for *cis* or *trans* 4-azo-5P lipids, respectively (see Fig 4b and Table 1). These observed kinetic phases are referred to as $k_{obs}1$-3. The fastest rate $k_{obs}1$ of ~ 7 s^{-1} was similar in both *trans* and *cis* 4-azo-5P, suggesting the same reaction event is occurring in both lipid states. This rate increased with increasing lipid (or vesicle) concentration and could be fit to a second order protein, lipid process (see Fig S6), thus indicating a reaction between MscL and lipid vesicles. $k_{obs}1$ thus likely represents the association of MscL with lipid vesicles. The amplitude of $k_{obs}1$ was over 10-fold greater for *cis* lipids, as opposed to *trans*. Since the amplitude is proportional to the amount of Trp, and thus protein, involved in the reaction event, this suggests that the initial association with vesicles is favoured by *cis* azo lipids.

$k_{obs}2$ was approximately an order of magnitude slower than $k_{obs}1$, being 0.1 s^{-1} and 0.03 s^{-1}, for *trans* and *cis* lipids, respectively. This $k_{obs}2$ rate is likely associated with monomer, monomer interactions and insertion into the vesicle bilayer. The amplitude of $k_{obs}2$ was 5-fold larger in *trans* lipids. A third very slow rate of small amplitude could be resolved for *trans* but not *cis* lipids.

The MscL(M42C-rhodamine) quenching kinetic data and increase in FRET associated with MscL(M42C-Alexa) assembly, were best fit by the sum of 3 phases; 2 first-order exponentials and an additional second-order rate constant (with respect to protein). The fastest exponential phase, $k_{obs}1$, agreed well with the MscL F93W data. This phase was observed for both rhodamine and FRET data with a higher amplitude in *cis* lipids, consistent with the MscL F93W data. The observation of FRET during $k_{obs}1$ suggests that monomer, monomer interactions occurs upon association with the vesicles, which could arise from an increase in monomer concentration at the vesicle surface. The rates resolved for $k_{obs}2$ are slightly different for the rhodamine and FRET measurements, being slower for the rhodamine data. This may represent the different sensitivities of the attached fluorescence tracers. The amplitude of $k_{obs}2$ is similar in *cis* and *trans* lipids for the rhodamine data, and ~ 2-fold larger for *cis*, than *trans*, lipids in the FRET data. Since both

these fluorescent tracers report primarily on monomer, monomer association, there seems to be a slightly greater association reported by FRET in *cis* rather than *trans* azo lipids. However, it is hard to use the kinetic data in a directly quantitative fashion. A much larger difference is observed in the $k_{obs}2$ amplitude in the F93W data, where the Trp fluorescence is significantly more quenched in *trans* rather than *cis* lipids. This is presumably because the F93W $k_{obs}2$ data is dominated by azo lipid quenching of the Trp during insertion into the lipids, as opposed to Trp self-quenching during monomer association. Thus we assign $k_{obs}2$ primarily to insertion of MscL into and across the lipid bilayer. This event is favoured by *trans* azo lipids. Further monomer, monomer association may also occur during $k_{obs}2$.

The third rate observed in the rhodamine and FRET data, $k_{obs}3$, exhibited pseudo second-order dependence on MscL monomer concentration, suggesting it is dominated by monomer, monomer association. Any higher order oligomerisation reactions will also be represented by this second order protein, protein reaction. The actual pentamer formation reaction mechanism may be complex. A pentamer is unlikely to form by 5 monomers reacting at once, but more likely to result from bimolecular reactions of lower order oligomers (e.g. a dimer and trimer). The amplitude of $k_{obs}3$ is greater in *trans* lipids as opposed to *cis*, in agreement with the increased FRET intensity observed in *trans* lipids (see Fig 5a). We suggest that $k_{obs}3$ reflects oligomerisation and formation of MscL oligomers, including functional pentamers, in the bilayer and that this process is favoured by *trans* lipids.

Overall, the kinetic experiments using the three different reporters, reveal three observed phases: $k_{obs}1$ correlates with initial association of SDS-MscL monomers with lipid vesicles and the data suggest that MscL associates more efficiently in lipid vesicles containing *cis* 4-azo-5P than *trans*. The observed kinetic rates, $k_{obs}2$ and $k_{obs}3$, primarily reflect insertion across the bilayer and formation of the pentamer, respectively. The associated amplitudes indicate that this insertion across and oligomerisation within the bilayer occurs more efficiently with *trans* 4-azo-5P present.

Photoisomerisation of azo lipids during re-assembly of MscL

Photoisomerisation of azo lipids was used to alter the bilayer properties during the MscL refolding reaction. The overall re-assembly of MscL occurs in approximately 8 mins in vesicles containing 10 % *cis* azo and >17 min with 10 % *trans* as determined by stopped flow measurements of folding kinetics. MscL(G22C) refolding was initiated by addition of SDS unfolded MscL at time, t=0. The azolipids were isomerized at time intervals (t_f) of 0.5, 1, 2, 4, 6, 8, 12 and 15 min, after the initiation of MscL refolding. Thus the isomerization state of the lipids was changed during MscL folding, after MscL had been allowed to fold for t_f min (see experimental scheme Fig S7). Isomerisation from *trans* to *cis* at time, t_f, was induced by illumination at 450 nm for 30 s, and *cis* to *trans* at 355 nm for 30 s (see Fig S2 for example spectra of 4-azo-5P after isomerisation). The folding reaction was left to reach completion in the absence of any additional illumination for a total of 60 min, after the initiation of folding. After this time, correctly folded, active channels, and thus successful refolding and assembly, were determined by the calcein dye release assay.

Final MscL activity, after completion of refolding, was similar for folding into vesicles with azolipids in the *cis* state throughout the experiment, as for those with the *trans* state throughout; i.e. with no isomerization at t_f during folding in either case (as observed in Fig 5b). However, changes were observed if the azo isomerization state was altered during folding. After initially refolding SDS-MscL into vesicles with *cis* lipids, an increase in the amount of dye release was observed when *cis* lipids were isomerized to *trans* at time t_f of 0.5 min after the initiation of folding, (an increase from the starting value in *cis* lipids of 16.9 ± 2.7 % to a value of 23.7 ± 2.5 % after isomerization to *trans*: see Fig 5c and d). This increase in dye release is consistent with an increase in the amount of re-assembled, functional channels. However, *cis* to *trans* isomerisation at t_f times >3 min after folding had little effect on the amount of dye release. Starting from the *trans* azolipid state, isomerisation from *trans* to *cis* after t_f of 0.5 min of folding had the opposite effect and reduced the activity of MscL channels (to 9.9 ± 0.5 % from the starting value in *trans* lipids of 18.3 ± 0.6 %). This reduction was observed for *trans* to *cis* isomerization at all times during folding; t_f = 0.5 to 15 mins after the initiation of folding. The experimental protocols utilised for functional assays and FRET assembly measurements in azo lipids are outlined in Figure S7.

Discussion

The pentameric channel MscL can be partially unfolded and refolded *in vitro*. Refolding MscL from a non-functional SDS-solubilised monomeric state into lipid vesicles results in recovery of native helical structure, oligomerisation and regain of functional channels, as shown by CD, FRET and calcein dye release. Kinetic studies with a variety of fluorescence tracers, suggest that this folding involves rapid association with lipid, followed by insertion across the bilayer together with oligomerisation and formation of active channels. The different stages of folding, and notably the efficiency of recovery of functional channels, can be manipulated by altering the surrounding lipid bilayer in a time-dependent manner.

The influence of lipid bilayers on membrane protein folding can be interpreted as arising from the differential lateral pressures exerted on the protein by the neighbouring lipids [10, 13, 44]. These lipid forces are a consequence of the elastic properties of the lipid membrane [7, 26, 45]. Monolayers of biological lipids exhibit different tendencies to curve towards water, depending on lipid headgroup and chain composition. Lipids such as phosphatidylcholine have a large radius of spontaneous curvature giving fairly flat monolayers that readily form the fluid lamellar, bilayer structure of the membrane. Lipids with smaller headgroups or increased chain unsaturation have smaller radii

of curvature and tend to form highly curved monolayers and thus non-bilayer, hexagonal phases. Incorporating such non-bilayer lipids into a bilayer lipid membrane increases the tendency for monolayer curvature. The monolayers, however, are forced flat in the bilayer, leading to an increase in stored curvature energy and alterations in the lateral pressure profile with an increase in the outward lipid chain pressure and a decrease in the headgroup region. Previous studies have shown that under such conditions the association of proteins into the headgroup locale is favoured, whilst the energy for inserting across the bilayer is greater due to the high chain pressure [2, 10, 11, 14, 17]. Here, we use photoisomerisable 4-azo-5P lipids to alter the lipid bilayer *in situ*, whilst maintaining a constant lipid composition. The more stable *trans* form of the azolipids readily incorporates into a lipid bilayer, but isomerisation to the *cis* form is likely to have a similar effect to increasing chain unsaturation by increasing monolayer curvature and chain lateral pressure, whilst decreasing headgroup pressures. Indeed previous reports indicate an increase in chain disorder with *cis* azolipids present as compared to *trans*, consistent with an increase in outward chain lateral pressure for *cis* lipids [37, 38]. We would thus predict that during folding, MscL would associate initially more favourably with *cis* azolipid bilayers (low headgroup pressure/high chain pressure), but that subsequent transmembrane insertion would be favoured by *trans* azolipids (low chain pressure) (see Fig 6). The observed folding kinetics support these predictions.

Three fluorescence probes were used, each reporting on different aspects of folding. Trp fluorescence reports mainly on the change in local environment and is dominated by quenching by the lipid azo group as the protein associates and inserts into the bilayer. Self-quenching between the individual Trps present on each monomer can also occur. Rhodamine fluorescence changes are dominated by self-quenching as monomers associate with each other and FRET reports primarily on monomer, monomer association and pentamer formation. For each kinetic tracer, the same rate constants are observed for bilayers containing either *cis* or *trans* lipids. Since rate constants are fingerprints for specific reactions, this shows that by maintaining the same chemical composition of the bilayer, the particular reactions reported by the fluorescence tracers are not altered by lipid isomerisation state and thus nor by the ensuing alterations in the bilayer forces. However, the amplitudes associated with each rate are dependent on lipid isomerisation. Amplitudes reflect the amount of protein undergoing the particular folding step. Table 1 shows that all 3 tracers resolve an increased amplitude for $k_{obs}1$ in *cis* lipids. $k_{obs}1$ is assigned to association of protein with the lipid bilayer. The Trp and rhodamine tracers report a greater than 10-fold increase in this amplitude, suggesting that more protein associates favourably with the lipid bilayer vesicles when the azo lipids are in the *cis* state. The observation of rhodamine and FRET during this phase also shows that some monomer association occurs, with more observed in *cis* than *trans* lipids. The amplitude of $k_{obs}2$ is significantly greater for Trp fluorescence kinetics in *trans* rather than *cis* lipids. We therefore suggest that this rate reports predominantly on transmembrane insertion across the bilayer, which will be favoured in *trans* lipids with their lower chain pressure, in line with previous kinetic observations on transmembrane helix insertion. Rhodamine fluorescence resolves similar amplitudes for this second kinetic phase in *cis* and *trans* lipids, whilst FRET reports a 2-fold larger amplitude in *cis* lipids. This suggests that monomer association which occurs as MscL inserts across the bilayer is largely independent of lateral pressure. The final second order rate, $k_{obs}3$, reflects mainly MscL monomer, monomer association with the FRET results suggesting that the MscL pentamer forms. This process is barely observed in Trp fluorescence, and is poorly resolved from $k_{obs}2$ in rhodamine fluorescence. More FRET is observed with *trans* lipids relative to *cis* (table 1 and Fig 5a) implying that the lower lateral chain pressure facilitates correct monomer, monomer association.

A model emerges for MscL folding where the relaxed headgroup pressure (and concomitant high chain pressure) of *cis* azo lipids favours initial association in the headgroup region of the bilayer. The later stages of transmembrane insertion and pentamer association, however, are favoured by the more relaxed chain pressure of *trans* lipids (see Fig 6). This confirms earlier suggestions that different stages of membrane protein folding and assembly are favoured by differing lateral pressures and bilayer mechanical properties [13, 44]. It also leads to a further prediction that can be tested due to the use of photoisomerisable lipids, which allow the bilayer properties to be changed during the folding process. We envisage that more active MscL channels will be recovered if the bilayer initially has the azolipids in the *cis* state that favours MscL association, with the lipids being subsequently altered to the *trans* state to favour the remaining insertion and assembly stages (see Fig 6). Fig 5d shows this to be the case; isomerisation from the favourable *cis* association state to the favourable *trans* insertion state after $k_{obs}1$ (i.e. after 0.5 mins) increases the number of active MscL channels. Conversely starting with the *trans* state and isomerising to *cis* after $k_{obs}1$, reduces MscL, bilayer association, insertion and assembly and thus the final number of active channels. In this latter scenario, it does not matter when the isomerisation to the *cis* state occurs (0.5 to 15 mins post folding initiation), since in all cases the initial, disfavoured association event is over and presumably competing aggregation and misfolding pathways dominate. In the case of the favourable *cis* to *trans* isomerisation during refolding, the increase in active channels only occurs when isomerisation is enacted between 0.5 and 3 mins after folding has started. This shows that after the insertion step $k_{obs}2$ is over, it is too late to isomerise and reduce the chain pressure to increase transmembrane insertion.

If there is no isomerisation of the starting lipid state, the same final activity is observed for both *cis* and *trans* lipids. However, FRET measurements suggest that more channels are recovered in *trans* lipids relative to *cis* (as determined by FRET). These results are consistent with channels in *cis* azolipid containing membranes being more active; as previously noted [46]. Thus, in *cis* lipids, fewer channels re-assemble, due to the increased chain

lateral pressure hindering insertion across the bilayer, but this raised pressure increases the activity of the channels that do re-form. This change in activity is consistent with previous studies on alpha-helical membrane proteins that exhibit altered activity as a result of changes in the membranes lateral pressure[47-49]. Additionally the results here agree with our previous observations that folding yield is dictated by the amount of protein that associates and inserts across the bilayer [10, 17, 50]. Thus, for example, increasing the bilayer chain pressure causes a reduction in the folding yield of bacteriorhodopsin that directly correlates with a decrease in the amount of protein inserting into the bilayer.

Conclusion

It is possible to partially denature MscL into partly unfolded monomers and recover the assembled channel *in vitro*. Manipulation of the lipid bilayer properties modulates the re-assembly reaction. The MscL folding reaction studied involves an initial lipid association followed by transmembrane insertion and oligomerisation, with the efficiency of these processes depending upon different bilayer properties. Association into the headgroup region is energetically favourable in bilayers with high chain but low headgroup pressure, whilst transmembrane insertion is favoured by a lower chain pressure. The dependence of different stages of folding and assembly on contrasting bilayer mechanical forces has implications for *in vivo* maturation of integral membrane proteins. Proteins often pass through different subcellular compartments with different lipid compositions and overall bilayer properties [52-54]. Hence, different folded or assembled states may be favoured with the final functional state only forming in the final membrane the protein resides in. The system used here of light activated lipids provide a generic means of manipulating the lipid bilayer during folding and thus altering the mechanical properties at specific stages of folding to afford fine control over different stages of the folding process.

Experimental

Wild type *E. coli* and mutant MscL were expressed and purified [51], and M42C MscL was labelled with either Rhodamine Red C2 maleimide, Alexa-488 maleimide, Alexa-568 maleimide or Alexa-647 maleimide (see Supplementary Information). MscL was electrophoresed on PAGE gels containing 0.2 M TRIS pH 8.45 and either 8 % acrylamide for native SDS-DDM-PAGE or 15 % acrylamide for SDS-PAGE. MscL was unfolded in low concentrations of SDS (8 mM), and subsequently diluted into lipid vesicles of 100 nm diameter. MscL containing lipid vesicles were isolated after refolding by flotation in a sucrose step gradient. Fluorescence was monitored for either Trp fluorescence (F93W MscL), FRET between donor and acceptor labels of M42C, or dye release as a result of channel opening [41, 42], and using stopped flow mixing for kinetic measurements.

DOPC/DOPG lipid vesicles were prepared and extruded to 100 nm diameter, as described in supplementary information. For azo lipid studies, lipid vesicles contained a maximum of 10% (w/v) of 4-azo-5P lipids, which were isomerised from *trans* to *cis* by illumination with an Nd-YAG laser for 30 s. *Cis* lipids were kept in the dark and isomerisation to *trans* occurred after 30 s illumination at 455 nm using a 3W LED light source. Isomerisation was verified by monitoring the absorbance of the lipid sample.

Acknowledgements

We acknowledge funding from The Leverhulme Trust (Project Grant F/00182/AW and Research Fellowship RF-2011-559 to PJB) and The Royal Society (for a Wolfson Research Merit Award to PJB). We also thank Eduardo Perozo for supplying the initial MscL construct, Andrew Orr-Ewing for use of a Nd-YAG laser and Elizabeth Bromley for assistance with AUC.

Figure and table legends

Figure 1: MscL structure showing sites of attachment of fluorescence tracers. An MscL monomer is shown in blue, with sites for introduction of Trp residues at position 93 shown in red and Cys residues for attachment of rhodamine or Alexa FRET dyes at position 42 shown in green, between transmembranes helices 1 and 2. The structure was generated from pdb 2OAR using PyMOL (DeLano Scientific).

Figure 2: Recovery of MscL secondary structure upon refolding from a partly denatured monomeric state in SDS. **a:** CD spectra of MscL at 10 μM after refolding into 0.21 and 0.87 mole fractions of SDS in DDM. A representative spectrum for fully folded MscL, i.e. as purified in 100 % DDM is shown in grey. Data are not smoothed. **b:** Increase in the negative 222 nm band at low SDS mole fraction is indicative of refolding and recovery of secondary structure upon removal of SDS. Representative errors are shown at low and high SDS, to 1 standard deviation for n=3. The solid line is the fit to an equilibrium two-state reaction. **c**: calculated α-helical content from data shown in B showing the increase in helicity upon removal of SDS. D: FRET acceptor emission from MscL M42C labeled with Alexa-488, Alexa-568 (one fluorophore per monomer) showing the increased emission observed in assembled pentameric MscL (low SDS) and decrease in dissociated monomeric MscL (high SDS), Error bars are 1 SD (for 3 measurements; n=3). The solid lines are the fit to an equilibrium two-state reaction

Figure 3: Recovery of activity as determined by release of calcein dye, upon refolding of SDS-denatured MscL into lipid vesicles. Raw data showing the increase in fluorescence with time after refolded MscL G22C channel is opened with MTSET. Separate traces show data for separate experiments with differen concentrations of MscL between 0 μM and 40 μM. Raw data are shown in black and single exponential fits as dashed grey. Background fluorescence at t=0 sec is set to 0 % dye release with 100 % determined by detergent solublisation of lipid vesicles. Data are representative examples from single experiments. Data were repeatable between experiments.

Figure 4: Azobenzene quenching of MscL Trp fluorescence. Quenching of Trp fluorescence emission upon folding MscL into lipid vesicles containing 2.5 % (w/w) *trans* 4-azo-5P lipids. **a**: fluorescence emission band of MscL F93W in the presence and absence of azo-lipid vesicles of 50 and 100 nm diameter. Maximal Trp fluorescence quenching was observed within ~300 sec after initiation of folding. The example spectra shown are 30 min after initiation of refolding. **b:** Kinetics of F93W fluorescence quenching upon folding into lipid vesicles containing 10 % azo lipid. All Trp fluorescence was observed to be quenched in both *cis* and *trans* azo lipid containing lipid vesicles. The dashed grey line shows a fit to the sum of two exponential components, with residuals from the difference between the data and fit shown below.

Figure 5: Influence of trans and cis azolipids on MscL pentamer formation and activity; a and b: measurements after MscL refolding and re-assembly; c and d, measurements during refolding a: FRET of Alexa-568/Alexa-647 MscL M42C refolded into lipid vesicles containing *cis* or *trans* conformations of 4-azo-5P. Dashed line: folding into cis 4-azo-5P, solid line: folding into *trans* 4-azo-5P. **b**: calcein dye release activity assay for MscL G22C refolded into lipid vesicles containing *trans* or *cis* 4-azo-5P containing lipid vesicles**.** Data are shown for MscL activity in t*rans* and cis lipids 60 min after the initiation of the folding reaction. Fits to a first order exponential (used for calculating maximum percent release) are shown as black lines. Dashed lines are control measurements in the absence of MscL illustrating no calcein leakage from the vesicles containing azo lipids; **c:** calcein dye release activity assay for MscL G22C refolded into lipid vesicles containing *trans* or *cis* 4-azo-5P containing lipid vesicles followed by isomerisation. Example data are shown for dye release from MscL after refolding into *cis* 4-azo-5P containing lipid vesicles followed by isomerisation to *trans* 4-azo-5P 30 sec after initiation of refolding (open circles) and *trans* 4-azo-5P followed by isomerisation to *cis* 30 sec after initiation of refolding (open diamonds). The folding reaction is left to continue until completion for a total of 60 min followed by measurement of channel activity by calcein dye release. The experimental scheme is shown in Fig S7. Fits to a first order exponential (used for calculating maximum percent release) are shown as black lines; **d:** Effect of azo-lipid isomerisation during MscL refolding on MscL activity. The x axis is the time after initiation of folding, t_f (MscL is added to lipid at t=0), at which lipid isomerisation is initiated. Open circles (*cis*-t*rans*); MscL initially refolded into *cis* azolipids with subsequent isomerisation to the *trans* form at the time points indicated. Open diamonds (*trans*-*cis*); MscL initially refolded into *trans* azolipids with subsequent isomerisation to cis. The MscL folding reaction proceeds for 60 min total at which point activity is determined by a calcein dye release assay. The y axis is the maximum percent release determined from a first-order exponential fit to the calcein release curve over time (as for example in fig 5b). MscL-G22C channels are opened by addition of MTSET. Controls in the absence of MscL, but with MTSET are shown for *trans* and *cis* lipids without isomerisation as open squares and open diamonds respectively to show the absence of dye release without MscL channel opening. Errors are 1 SEM for n=3).

Figure 6: Schematic showing favourable MscL folding conditions by isomerisation of azolipids during folding. The low headgroup pressure of bilayers containing cis azo lipids favours initial association of the protein. Subsequent isomerisation of *trans* lipids decreases the lateral chain pressure which favours transmembrane insertion. MscL is shown as black rectangles to represent the α helices. High lipid lateral pressure is indicated by red shading and low pressure in grey. MscL is folded from a dentured monomeric state in SDS (not shown). The association event of SDS-MscL with the vesicles (reported by $k_{obs}1$) is also not shown. The reactions reflected in the observed kinetic rates $k_{obs}2$ and $k_{obs}3$ are indicated; $k_{obs}2$ reflects insertion of MscL across the bilayer together with some monomer formation and $k_{obs}3$ monomer, monomer association to form higher order MscL oligomers and pentamer.

Table 1: Folding kinetics of MscL in azolipid vesicles. Vesicles comprised 40 % DOPC, 50 % DOPG and 10 % cis or *trans* 4-azo-5P lipids (w/v). Trp fluorescence data were fit to the sum of 2 or 3 first order rate constants (thus $k_{obs}3$ has units of s^{-1}). Rhodamine and FRET data were fit to the sum of 2 first order rates one 2nd order ($k_{obs}3$). Amplitudes are shown in parenthesis and are raw data values in V, with a positive amplitude indicating a decrease in Trp and rhodamine fluorescence and a negative amplitude for the increase in FRET. These are comparable with the same measurement, but not directly comparable between the different tracers, although the same protein and lipid concentrations were used in each case. Similarly, the units for $k_{obs}3$ are $V^{-1}.s^{-1}$, to avoid assumptions in conversion of the signal amplitude in V to concentration of MscL. First standard deviation errors from at least 3 measurements for Trp and rhodamine fluorescence are < ± 5 % and < ± 10 % of the magnitudes of the rate constant and amplitude, respectively. Errors for FRET are < ± 10% and < ± 20% of the magnitudes of the r ate constant and amplitude, respectively.

‡**Abbreviations.** AUC, analytical ultracentrifugation; 4-Azo-5P, di-(5-[[4-(4-butylphenyl)azo]phenoxy]pentyl)phosphate; CD, circular dichroism; CMC, Critical micellar concentration; DDM, dodecylmaltoside; DGK, Diacylglycerol kinase; ; DOPC, L-□-1,2-dioleoyl-sn-glycero-3-phosphocholine; DOPG, L-□-1,2-dioleoyl-sn-glycero-3-phosphoglycerol; FRET, Förster resonance energy transfer; MscL, Mechanosensitive channel of large conductance; MTSET, trimethylammonium ethyl methanethiosulfonate; PAGE, polyacrylamide gel electrophoresis; PC, phosphatidylcholine; SDS, sodium dodecylsulfate; SEM, standard error of the mean

References

1. K. Charalambous, P. J. Booth, R. Woscholski, J. M. Seddon, R. H. Templer, R. V. Law, L. M. Barter and O. Ces, *J Am Chem Soc*, 2012, **134**, 5746-5749.
2. G. S. Attard, R. H. Templer, W. S. Smith, A. N. Hunt and S. Jackowski, *Proc. Natl. Acad. Sci. USA*, 2000, **97**, 9032-9036.
3. S. M. Bezrukov, *Curr. Op. Coll. Int. Sci.*, 2000, **5**, 237-243.
4. S. M. Gruner, *Proc. Natl. Acad. Sci. USA*, 1985, **82**, 3665-3669.
5. A. G. Lee, *Biochemical Society transactions*, 2011, **39**, 761-766.
6. A. G. Lee, *Molecular Biosystems*, 2005, **1**, 203-212.
7. E. van den Brink-van der Laan, J. A. Killian and B. de Kruijff, *Biochim Biophys Acta*, 2004, **1666**, 275-288.
8. N. Jenne, K. Frey, B. Brugger and F. T. Wieland, *J Biol Chem*, 2002, **277**, 46504-46511.
9. J. K. Vanslyke, C. C. Naus and L. S. Musil, *Mol Biol Cell*, 2009, **20**, 2451-2463.
10. S. J. Allen, A. R. Curran, R. H. Templer, W. Meijberg and P. J. Booth, *J. Mol. Biol.*, 2004, **342**, 1293-1304.
11. W. Meijberg and P. J. Booth, *J. Mol. Biol.*, 2002, **319**, 839-853.
12. P. J. Booth, R. H. Templer, J. W. Meijberg, S. J. Allen, M. Lorch and A. R. Curran, *Crit. Rev. Biochem. Mol. Biol*, 2001, **36**, 501-603.
13. P. J. Booth, *Curr Opin Struct Biol*, 2005, **15**, 435-440.
14. W. Meijberg and P. J. Booth, *J Mol Biol*, 2002, **319**, 839-853.
15. E. L. Compton, N. A. Farmer, M. Lorch, J. M. Mason, K. M. Moreton and P. J. Booth, *J Mol Biol*, 2006, **357**, 325-338.
16. S. J. Allen, A. R. Curran, R. H. Templer, W. Meijberg and P. J. Booth, *J Mol Biol*, 2004, **342**, 1279-1291.
17. S. J. Allen, A. R. Curran, R. H. Templer, W. Meijberg and P. J. Booth, *J Mol Biol*, 2004, **342**, 1293-1304.
18. A. M. Seddon, M. Lorch, O. Ces, R. H. Templer, F. Macrae and P. J. Booth, *J Mol Biol*, 2008, **380**, 548-556.
19. M. Lorch and P. J. Booth, *J Mol Biol*, 2004, **344**, 1109-1121.
20. M. Wikstrom, A. A. Kelly, A. Georgiev, H. M. Eriksson, M. R. Klement, M. Bogdanov, W. Dowhan and A. Wieslander, *J Biol Chem*, 2009, **284**, 954-965.
21. W. Dowhan and M. Bogdanov, *Annu Rev Biochem*, 2009, **78**, 515-540.
22. F. N. Barrera, M. L. Renart, J. A. Poveda, B. de Kruijff, J. A. Killian and J. M. Gonzalez-Ros, *Biochemistry*, 2008, **47**, 2123-2133.
23. J. A. Encinar, M. L. Molina, J. A. Poveda, F. N. Barrera, M. L. Renart, A. M. Fernandez and J. M. Gonzalez-Ros, *FEBS Lett*, 2005, **579**, 5199-5204.
24. F. I. Valiyaveetil, Y. Zhou and R. MacKinnon, *Biochemistry*, 2002, **41**, 10771-10777.
25. P. Moe and P. Blount, *Biochemistry*, 2005, **44**, 12239-12244.
26. D. Marsh, *Biophysical journal*, 2007, **93**, 3884-3899.
27. P. Blount, S. I. Sukharev, P. C. Moe, M. J. Schroeder, H. R. Guy and C. Kung, *The EMBO journal*, 1996, **15**, 4798-4805.
28. I. Iscla, R. Wray and P. Blount, *Protein sci*, 2011, **20**, 1638-1642.
29. G. Chang, R. H. Spencer, A. T. Lee, M. T. Barclay and D. C. Rees, *Science*, 1998, **282**, 2220-2226.
30. K. Yoshimura, J. Usukura and M. Sokabe, *Proc Natl Acad Sci U S A*, 2008, **105**, 4033-4038.
31. M. Ornatska, S. E. Jones, R. R. Naik, M. O. Stone and V. V. Tsukruk, *J Am Chem Soc*, 2003, **125**, 12722-12723.
32. J. H. Folgering, J. C. Wolters and B. Poolman, *Protein sci*, 2005, **14**, 2947-2954.
33. Z. Liu, C. S. Gandhi and D. C. Rees, *Nature*, 2009, **461**, 120-124.
34. C. E. Price, A. Kocer, S. Kol, J. P. van der Berg and A. J. Driessen, *FEBS Lett*, 2011, **585**, 249-254.
35. C. Berrier, I. Guilvout, N. Bayan, K. H. Park, A. Mesneau, M. Chami, A. P. Pugsley and A. Ghazi, *Biochim Biophys Acta*, 2011, **1808**, 41-46.
36. J. H. Folgering, J. M. Kuiper, A. H. de Vries, J. B. Engberts and B. Poolman, *Langmuir*, 2004, **20**, 6985-6987.
37. J. M. Kuiper, M. C. Stuart and J. B. Engberts, *Langmuir*, 2008, **24**, 426-432.
38. E. H. Backus, J. M. Kuiper, J. B. Engberts, B. Poolman and M. Bonn, *The journal of physical chemistry. B*, 2011, **115**, 2294-2302.
39. A. Kocer, M. Walko, W. Meijberg and B. L. Feringa, *Science*, 2005, **309**, 755-758.
40. B. Corry, P. Rigby, Z. W. Liu and B. Martinac, *Biophysical journal*, 2005, **89**, L49-51.
41. A. M. Powl, J. M. East and A. G. Lee, *Biochemistry*, 2003, **42**, 14306-14317.
42. A. M. Powl, J. M. East and A. G. Lee, *Biochemistry*, 2008, **47**, 4317-4328.
43. A. Kocer, M. Walko and B. L. Feringa, *Nat Protoc*, 2007, **2**, 1426-1437.
44. P. J. Booth, *Curr. Opin. Struct. Biol.*, 2005, **15**, 435-440.
45. W. Helfrich, *Z. Naturforsch*, 1973, **28c**, 693-703.
46. J. H. Folgering, J. M. Kuiper, A. H. de Vries, J. B. Engberts and B. Poolman, *Langmuir*, 2004, **20**, 6985-6987.
47. A. V. Botelho, N. J. Gibson, R. L. Thurmond, Y. Wang and M. F. Brown, *Biochemistry*, 2002.
48. J. D. Pilot, M. East and A. G. Lee, *Biochemistry*, 2001, **40**, 14891-14897.
49. C. Van der Does, J. Swaving, W. van Klompenburg and A. J. M. Driessen, *J. Biol. Chem.*, 2000, **275**, 2472-2478.
50. A. R. Curran, R. H. Templer and P. J. Booth, *Biochemistry*, 1999, **38**, 9328-9336.
51. D. M. Cortes, L. G. Cuello and E. Perozo, *J. Gen. Physiol.*, 2001, **117**, 165-180.
52. A. Y. Andreyev, E. Fahy, Z. Guan, S. Kelly, X. Li, J. G. McDonald, S. Milne, D. Myers, H. Park, A. Ryan, B. M. Thompson, E. Wang, Y. Zhao, H. A. Brown, A. H. Merrill, C. R. Raetz, D. W. Russell, S. Subramaniam and E. A. Dennis, *J Lipid Res*, 2010, **51**, 2785-2797.
53. R. Schneiter, B. Brugger, R. Sandhoff, G. Zellnig, A. Leber, M. Lampl, K. Athenstaedt, C. Hrastnik, S. Eder, G.

Daum, F. Paltauf, F. T. Wieland and S. D. Kohlwein, *J Cell Biol*, 1999, **146**, 741-754.

54. E. Zinser, C. D. Sperka-Gottlieb, E. V. Fasch, S. D. Kohlwein, F. Paltauf and G. Daum, *J Bacteriol*, 1991, **173**, 2026-2034.

Figure 1

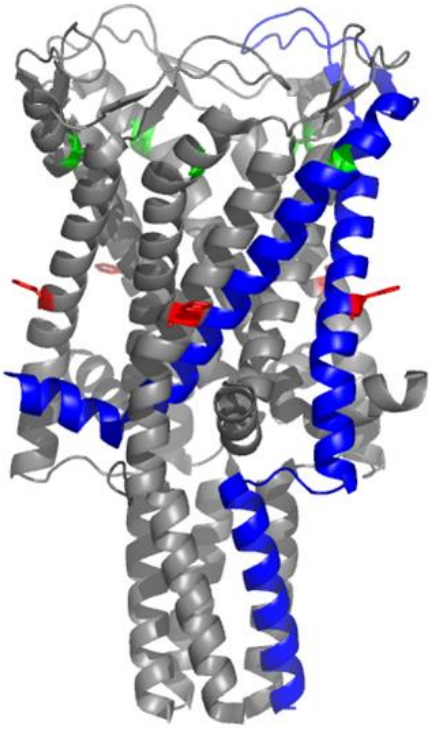

Figure 2

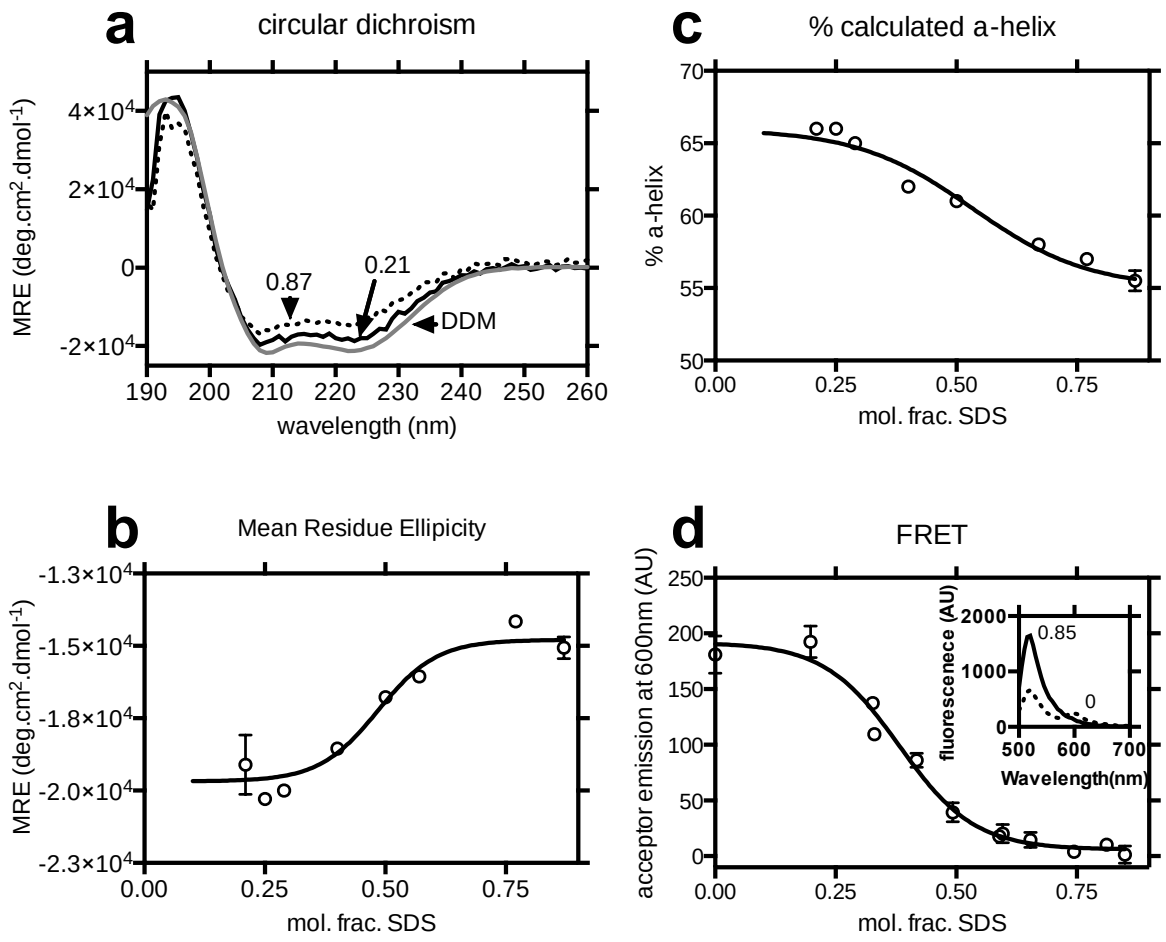
a
circular dichroism
MRE (deg.cm2.dmol-1)
4×10^4
2×10^4
0
-2×10^4
0.87
0.21
DDM
190 200 210 220 230 240 250 260
wavelength (nm)
c
% calculated a-helix
% a-helix
70
65
60
55
50
0.00 0.25 0.50 0.75
mol. frac. SDS
b
Mean Residue Ellipicity
MRE (deg.cm2.dmol-1)
-1.3×10^4
-1.5×10^4
-1.8×10^4
-2.0×10^4
-2.3×10^4
0.00 0.25 0.50 0.75
mol. frac. SDS
d
FRET
acceptor emission at 600nm (AU)
250
200
150
100
50
0
0.00 0.25 0.50 0.75
mol. frac. SDS
fluorescenece (AU)
2000
1000
0
0.85
0
500 600 700
Wavelength(nm)

Figure 3

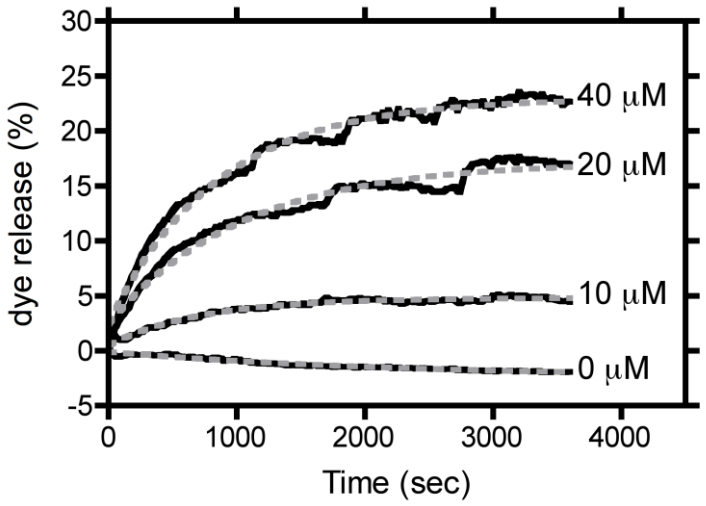
30
25
20
15
10
5
0
-5
dye release (%)
0
1000
2000
3000
4000
Time (sec)
40 μM
20 μM
10 μM
0 μM

Figure 4

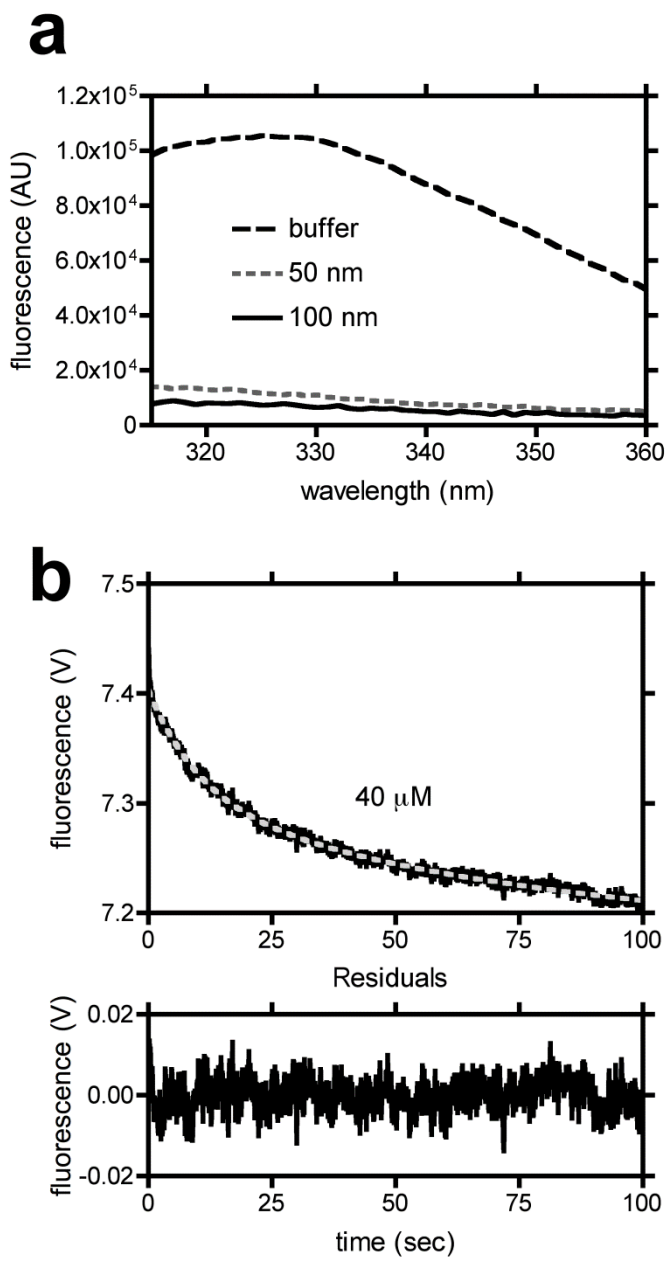
a
1.2x10^5
1.0x10^5
8.0x10^4
6.0x10^4
4.0x10^4
2.0x10^4
0
fluorescence (AU)
buffer
50 nm
100 nm
320
330
340
350
360
wavelength (nm)
b
7.5
7.4
7.3
7.2
fluorescence (V)
40 μM
0
25
50
75
100
Residuals
0.02
0.00
-0.02
fluorescence (V)
0
25
50
75
100
time (sec)

Figure 5

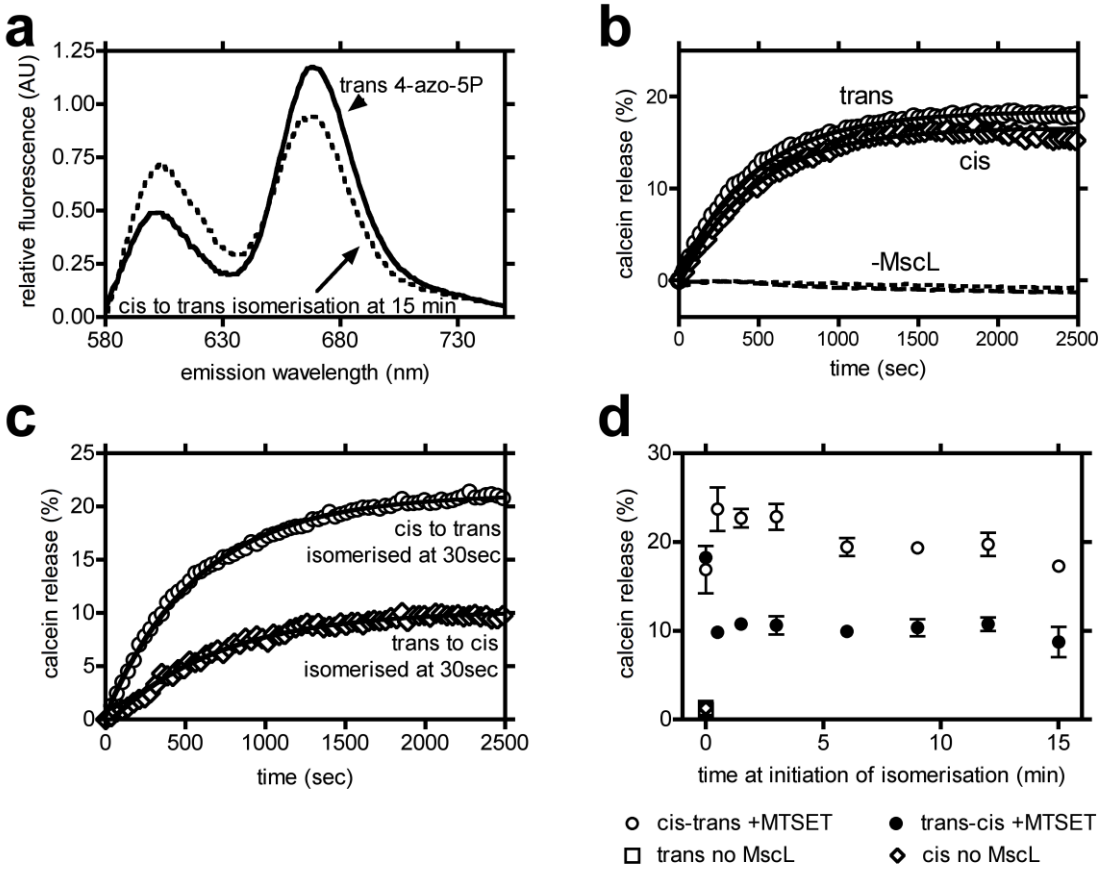
a
relative fluorescence (AU)
1.25
1.00
0.75
0.50
0.25
0.00
580
630
680
730
emission wavelength (nm)
trans 4-azo-5P
cis to trans isomerisation at 15 min
b
calcein release (%)
20
10
0
trans
cis
-MscL
0
500
1000
1500
2000
2500
time (sec)
c
calcein release (%)
25
20
15
10
5
0
cis to trans
isomerised at 30sec
trans to cis
isomerised at 30sec
0
500
1000
1500
2000
2500
time (sec)
d
calcein release (%)
30
20
10
0
0
5
10
15
time at initiation of isomerisation (min)
cis-trans +MTSET
trans-cis +MTSET
trans no MscL
cis no MscL

Figure 6

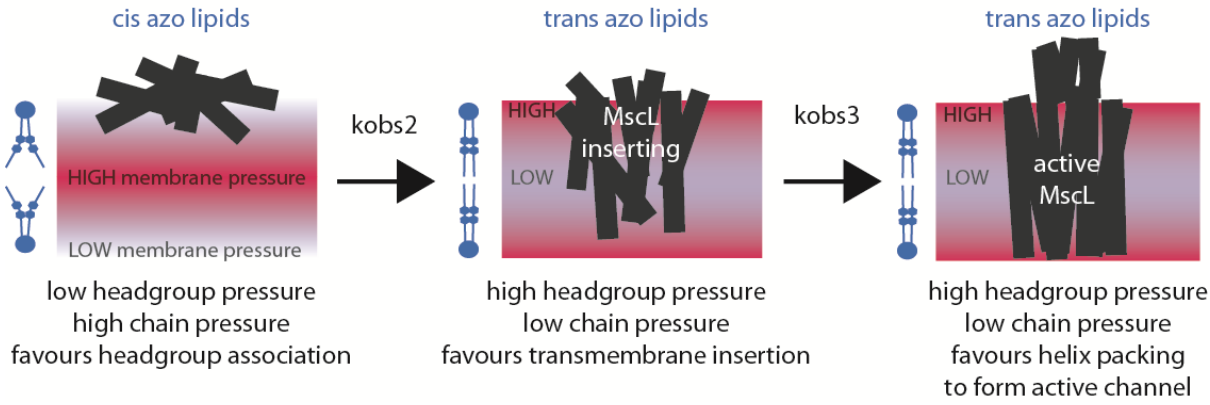
cis azo lipids
trans azo lipids
trans azo lipids
HIGH membrane pressure
LOW membrane pressure
kobs2
HIGH
LOW
MscL inserting
kobs3
HIGH
LOW
active MscL
low headgroup pressure
high chain pressure
favours headgroup association
high headgroup pressure
low chain pressure
favours transmembrane insertion
high headgroup pressure
low chain pressure
favours helix packing
to form active channel

Table 1

Measurement	**Azolipid isomerisation state**	**Observed kinetic phases**		
		$k_{obs}1$ (s^{-1})	**$k_{obs}2$ (s^{-1})**	**$k_{obs}3$ ($V^{-1}s^{-1}$)**
Trp fluorescence	cis	**7.7** (1.48 V)	**0.028** (0.05 V)	not resolved
	trans	**7.2** (0.13 V)	**0.10** (0.26 V)	**0.0065 s^{-1}** (0.25 V)
Rhodamine fluorescence	cis	**6.6** (1.2 V)	**0.045** (0.14 V)	**0.019** (0.17 V)
	trans	**1.6** (0.11 V)	**0.078** (0.18 V)	**0.019** (0.65 V)
FRET	cis	**14** (-1.5 V)	**0.24** (-1.0 V)	**0.0010** (-2.1 V)
	trans	**9.6** (-0.64 V)	**0.17** (-0.47 V)	**0.0029** (-4.6V)
Assignment of kinetic phase		*Association of MscL with lipid vesicles together with MscL monomer, monomer association*	*Insertion of MscL into and across bilayer*	*MscL oligomer/pentamer formation*